Optics of the eye and its impact in vision: A tutorial

Article *in* Advances in Optics and Photonics · September 2014

DOI: 10.1364/AOP.6.000340

1 author:

Pablo Artal
University of Murcia
413 PUBLICATIONS **12,731** CITATIONS

SEE PROFILE

Optics of the eye and its impact in vision: a tutorial

Pablo Artal

Laboratorio de Óptica, Instituto Universitario de Investigación en Óptica y Nanofísica, Universidad de Murcia, Campus de Espinardo (Edificio 34), E-30100 Murcia, Spain (pablo@um.es)

Received August 6, 2014; revised September 8, 2014; accepted September 9, 2014; published September 24, 2014 (Doc. ID 220531)

The human eye is a relatively simple optical instrument. This limits the quality of the retinal image affecting vision. However, the neural circuitry seems to be exquisitely designed to match the otherwise limited optical capabilities, providing an exceptional quality of vision. In this tutorial article, the main characteristics of the eye's geometry and optics will first be reviewed. Then, their impact on vision under a variety of normal conditions will be discussed. The information gathered here should serve both those readers interested in basic vision and physiological optics and those more interested in related applications.

OCIS codes: (330.0330) Vision, color, and visual optics; (080.0080) Geometric optics; (120.0120) Instrumentation, measurement, and metrology
http://dx.doi.org/10.1364/AOP.6.000340

Optics of the eye and its impact in vision: a tutorial

Pablo Artal

1. Introduction

The human eye is an extremely robust, and rather simple, optical instrument. It is composed of only two positive lenses, the cornea and the crystalline lens, that project images of the world into the retina initiating the visual process. Compared with artificial optical systems, often formed by many lenses to improve image quality when working over a range of angles and wavelengths, the eye is much simpler, but well adapted to the requirements of the visual system. The eye has to form high-resolution images of a large field of view for objects placed at different distances using transparent living tissue, instead of glass. These are demanding tasks to be accomplished. An important assumption is that vision will be good only if the images formed on the retina have sufficient quality. If the retinal images are blurred, the visual system will not function properly and vision will be poor. Of course, the opposite is not true since many retinal and neural diseases may impair vision even when a decent retinal image is formed.

It is not very surprising that for a majority of persons, the eye is the most important optical system. And as often happens with the most important things, it is usually as revered as neglected. For optical scientists and engineers, the eye is very commonly regarded as so simple and well understood compared to artificial optical systems that it does not merit much attention. I still remember vividly when I had to decide the topic for my own Ph.D. thesis work. A physics professor told me that I should not waste my time and juvenile efforts in pursuing studies on something "*as simple and unexciting as the eye's optics*." I am glad now that I did not follow his advice, and I started my thesis developing instruments to measure the image quality of the human eye. I am mentioning this personal anecdote simply to insist that the optics of the eye may not be fully appreciated by the community of physical and engineering optical scientists. In this context, I prepared this tutorial with the main following objectives in mind:

(i) to revise and compile our basic understanding on the optics of the eye;
(ii) to list systematically how optics limit vision for different conditions; and
(iii) to show that a better understanding of the eye's optics permits improvement of vision correction techniques.

2. The Eye as an Optical Instrument

2.1 Structure and Geometry of the Eye

The eye in adult humans is approximately a sphere of around 24 mm in diameter. Externally it is covered by a resistant and flexible tissue called the sclera, except in the anterior part where the transparent cornea allows the light to pass into the

eye. Internal to the sclera are two other layers: the choroid, to provide nutrients, and the retina, where the light is absorbed by the photoreceptors after image formation. The eye moves due to the action of six external muscles, permitting fixation and scanning of the visual environment. The light reaching the eye is first refracted by the cornea, a thin transparent layer free of blood vessels of about 12 mm in diameter and around 0.55 mm thickness in the central part. An aqueous tear film on the cornea ensures that the first optical surface is smooth to provide the best image quality. After the cornea, the anterior chamber is filled with the aqueous humor, a water-like substance. The iris, two sets of muscles with a central hole whose size depends on its contraction, acts as a diaphragm with characteristic color depending on the amount and distribution of pigments. The aperture is the opening in the center of the iris, and limits the amount of light passing into the eye. The entrance pupil is the image of the iris through the cornea, and the exit pupil is the image of the aperture through the lens. The aperture size changes with the ambient light, from less than 2 mm in diameter in bright light to more than 8 mm in the dark. The pupil controls retinal illumination and limits the rays entering the eye, affecting the retinal image quality. After the iris, the crystalline lens combines with the cornea to form the images on the retina. While the cornea is a lens with fixed optical power, the crystalline lens is an active optical element. It changes its shape, modifying its optical power and, therefore, the whole eye's power. This is the basis of the mechanism of accommodation that allows the eye to focus on objects placed at different distances. The lens is surrounded by an elastic capsule and attached by ligaments called zonules to the ciliary body. The action of the muscles in the ciliary body permits the lens to increase or decrease power. The ability to keep near objects in focus declines continuously with age until reaching presbyopia, when subjects are unable to accommodate.

After the light is refracted by the lens, it enters the posterior chamber filled with the transparent vitreous humor and then reaches the retina. This is a thin layer of neural tissue covering the back of the eyeball, acting as a screen where images are formed and the light is converted into electrochemical signals. The human retina has a central area, the fovea, where photoreceptors are densely packed to provide the highest resolution. The eyes move continuously to fixate the desired details into the fovea. The peripheral parts of the retina render lower resolution but specialize in movement and object detection in the visual field. The typical field covered by the eye is quite large compared with most artificial optical systems—at least $160\ \text{deg} \times 130\ \text{deg}$.

Figure 1 is a schematic representation of the eye with the main geometrical and optical information. These data, distances (red numbers), radii of curvature (black numbers), and refractive indices (blue numbers), have to be understood as average values.

As will be discussed later, every eye is intrinsically unique, but these average values are useful for the purpose of generalization. The cornea is approximately a spherical section with an anterior radius of curvature of 7.8 mm, posterior radius of curvature of 6.5 mm, and refractive index of 1.3771. Since the largest difference in refractive index occurs from the air to the cornea (actually the tear film), this accounts for most of the refractive power of the eye, on average over 70%. The lens is a biconvex lens with radii of curvature of 10.2 and −6.0 mm for the anterior and posterior surfaces. The internal structure of the lens is layered, which produces a non-homogeneous refractive index, higher in the center than in

Figure 1

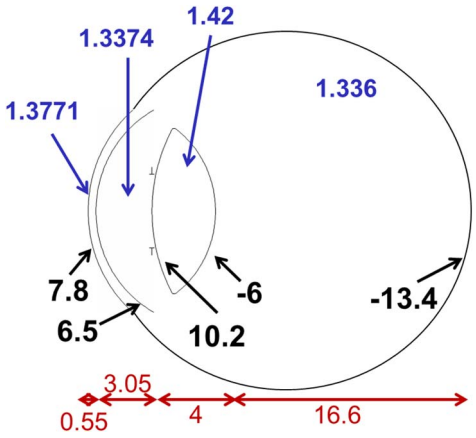

Schematic representation of the eye with the main geometrical and optical information. Refractive indices (blue), curvature radii (black), and distances (red) in mm.

the periphery and with an equivalent value of 1.42. The refractive indices of the aqueous and vitreous humors are 1.3374 and 1.336, respectively.

An average eye with these distances—3.05, 4, and 16.6 mm for the anterior chamber, lens, and posterior chamber, respectively—will have an axial length of 24.2 mm and will image distant objects precisely in focus into the retina. This ideal situation is called emmetropia. However, most eyes have neither the adequate optical properties nor the dimensions to achieve perfect focus; they are affected by optical refractive errors. In these cases, the images formed in the retina are blurred, typically imposing a lower limit to visual perception. Refractive errors are classified as myopia, when the images of distant objects are focused in front of the retina, and hypermetropia, when distant objects are focused behind the retina. In addition, in every person the eye is not rotationally symmetric as ideally described here. A common manifestation of these facts is the presence of astigmatism: the retinal image of a point source consists of two perpendicular lines at different focal distances. Even in the case of eyes free of any refractive error, without defocus and astigmatism, they do not produce perfect images. The retinal image of a point source would not be another point, but an extended distribution of light due to the high-order optical aberrations. This will be reviewed in detail in the following sections.

Unlike most artificial systems, the eye is not a centered optical system since the ocular surfaces are not spherical in shape and they are not perfectly aligned. In

Figure 2

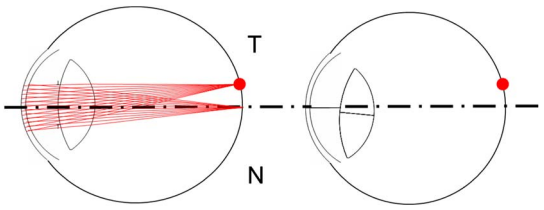

Examples of location of the fovea (represented by the red circle) outside the optical axis and a possible decentering/tilt of the crystalline lens (right figure).

addition, the area of the retina providing the highest resolution, the fovea, is decentered temporally (in average around 5 deg), and the lens can also be tilted and/or decentered with respect to the cornea (see schematics of Fig. 2).

2.2. Axes and Angles in the Eye

Figure 2 introduces the need for clarifying the definitions of the axes and angles involved in the eye. This is usually confusing, not because of an inherent difficulty, but due to the multiple definitions and names that can be found in the literature. I will follow here the definition of Le Grand and El Hage [1]. Figure 3 should help with the identification of the definitions provided below.

As I mentioned, there is not an optical axis for the eye, so instead we define two axes related to physiological features. The pupillary axis is the line perpendicular to the cornea that intersects the center of the entrance pupil. The line of sight connects the fixation point in the object space to the center of the entrance pupil (and the center of the exit pupil with the fovea). These axes (line of sight and pupillary axis) may be considered approximations to the optical axis and the visual axis of the eye, respectively (the visual axis connects the fixation point to the fovea via the nodal points). The angle kappa (κ) is the angular distance (in the object space) between the line of sight and the pupillary axis. It should be noted that in the literature this is also often referred as angle lambda (λ). It is not helpful that the same angle is referred in the literature with two different names: kappa and lambda. Those readers interested in some of the historical reasons for the names issues may read Appendix A. I prefer to use the term kappa (and this will be followed here). In practical terms, the two angles are nearly identical, according to Le Grand and El Hage [1]: "*It seems unnecessary to distinguish this (angle lambda) from kappa, which is practically equal to it when the point of fixation is not very close to the eye*."

Typically, the angle kappa can be determined for a particular eye using the Purkinje images. These are the reflections in the surfaces of the cornea and lens when the eye is illuminated with a source (Fig. 4 represents a classic view of the phenomenon by Helmholtz).

In our laboratory, we developed an instrument based in this principle [2]. To estimate the angle kappa, we measure the displacement of the first Purkinje image (reflection from the anterior corneal surface) with respect to the pupil center as a function of the fixation angle of the eye looking at a target. To generate the corneal reflex, we projected into the eye a semicircular arrangement of infrared

Figure 3

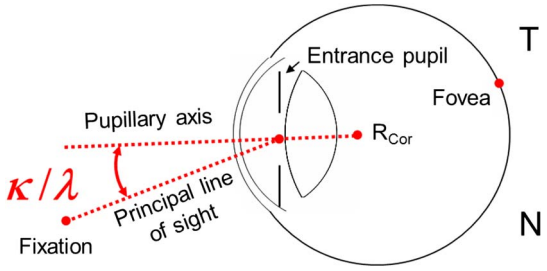

Schematic representation of the main axes and angles commonly defined in the eye.

Figure 4

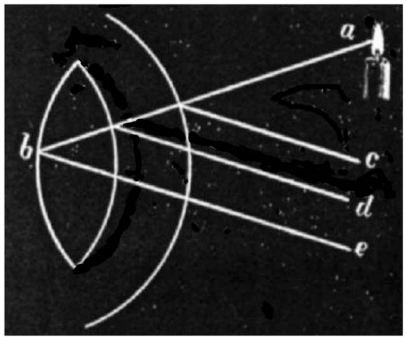

Drawing from Helmholtz representing the Purkinje reflections in the anterior surfaces of the eye (cornea and lens).

LEDs, placed at a fixed axial distance from the eye's entrance pupil. This was achieved by aligning the line of sight of the eye with the optical axis of the experimental setup, and then focusing the pupil plane (moving axially the head of the subject) on a CCD camera with a telecentric objective. We considered the array of LEDs as a collection of point light sources, each subtending a different angle with respect to the line of sight. The eye was required to fixate a single central stimulus, and a picture of the anterior pupil plane with the first Purkinje image of the array of LEDs was recorded to estimate angle kappa (Fig. 5). In the image, a semi-ellipse was adjusted to the semicircular corneal reflex and a full ellipse to the pupil edge to measure the longitudinal x- and y-positions of each component of the corneal reflex (LED images) with respect to the pupil center. These positions were linearly correlated with the angular positions subtended by the corresponding original illuminating LED, using previously tested fitting constants. We estimated angle kappa as the extrapolated angle that overlapped the center of the pupil and the corneal reflex.

Figure 6 shows the values of kappa angle, in a polar representation, measured with this instrument for a group of normal eyes. This shows the inherent

Figure 5

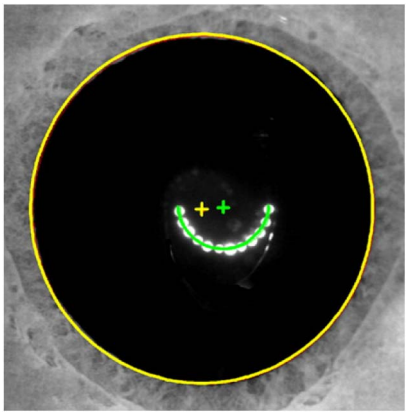

First Purkinje image of a semicircle of LEDs and its center (green cross), and the pupil edge and its center (yellow cross). From this type of image, information on angles and lens tilt and decentration is obtained.

The average eye has an angle kappa of around 4 deg horizontally in the temporal direction and is centered vertically.

variability of ocular data, in this case for the kappa angle. On average, angle kappa is around 4 deg horizontally in the temporal direction. However, some eyes may even have a negative kappa angle (toward the nasal direction), and in others it can be as large as 8 deg in the temporal direction. The same variability appears in the vertical direction, ranging from 4 deg superior to inferior, although, on average, eyes are vertically centered. This is just one simple, but representative, example that average data for the eye are a clear oversimplification, and therefore customized modeling based in real personal data is preferred.

Figure 6

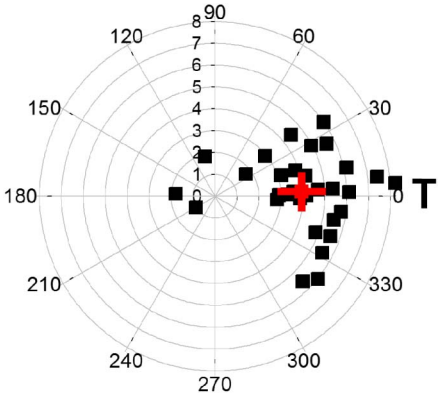

Kappa angle for a group of normal subjects. The red symbols indicate the average value and standard deviation.

Figure 7

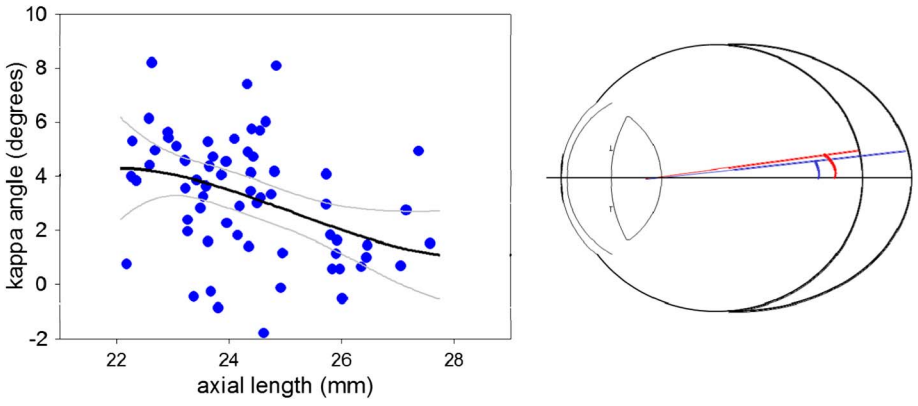

Kappa angle in a group normal subjects with different values of axial length. Longer eyes (typically myopic) have smaller angle kappa than shorter eyes (hyperopes). The diagram on the right presents a simple explanation of the angular dependence with axial length. Adapted from J. Opt. Soc. Am. A **24**, 3274–3283 (2007) [3].

The data of Fig. 6 were obtained for a group of nearly emmetropic subjects. Angle kappa depends on the axial length, with hyperopic eyes tending to have a larger angle kappa than myopic eyes (see left panel in Fig. 7). This can be explained by a simple model of axial growth of the eye. One of the mechanisms for the development of myopia is an abnormal axial growth of the eye. Therefore, it is expected that the fovea would remain relatively unchanged in its position with little migration in this direction, since the main growth of the eye is axial. Assuming that the foveal position is stable in the growing eye (see Fig. 7, right panel) and also that the change in the approximate nodal points of the eye is small in comparison to the change in the axial position of the retina, a simple model of how angle kappa might change with the axial length of the eye can be deduced [3].

2.3. Retinal Image Quality

Although it is outside the main scope of this tutorial, for the sake of completeness, I will briefly review some basic concepts on image formation. For those readers interested in more detail, these textbooks, among many others, are a good starting point [4,5]. The wave aberration is a function that characterizes the image forming properties of any optical system. It is defined as the difference between the perfect (spherical) and the real wavefront for every point over the pupil. For example, an eye without aberrations has a constant or null wave aberration and forms a perfect retinal image of a point source (called the Airy disk, which depends only on the pupil diameter and the mean wavelength). However, an eye with aberrations produces a more extended, and generally asymmetric, retinal image. This image of a point source is called the point-spread function (PSF). Although the wave aberration can be a quite complicated two-dimensional function, it can be decomposed through polynomials in a sum of pure aberration modes. The lower order terms correspond to the well-known defocus and astigmatism, while the following terms are some of the higher order aberrations: coma, spherical aberration, triangular astigmatism, etc. A convenient and widely used way to decompose the wave aberration is the Zernike polynomial expansion [6]. From the PSF, a useful single image quality parameter, the Strehl ratio, is defined as the ratio between the peak intensity of the eye's PSF and that of the aberration-free (diffraction-limited) PSF. In addition, by performing a convolution operation of an object and the eye's PSF, it is possible to predict the retinal image of any scene.

Several factors are responsible for the degradation of the retinal images: diffraction of the light in the eye's pupil, optical aberrations, and intraocular scattering. Diffraction blurs the images formed through instruments with a limited aperture due to the wave nature of the light. The effect of diffraction in the eye is small and actually noticeable only with small pupils. The impact of ocular aberrations in image quality is more significant for larger pupil diameters. The aperture of the eye ranges from $f/8$ to $f/2$, values that can be compared with the typical values in a camera objective. The amount of higher order aberrations for a

> On average for a 5 mm diameter pupil, the amount of aberrations in normal eyes, expressed as the root mean squared of the wave aberration, is 0.25 μm (approximately equivalent to 0.25 D of defocus).

Figure 8

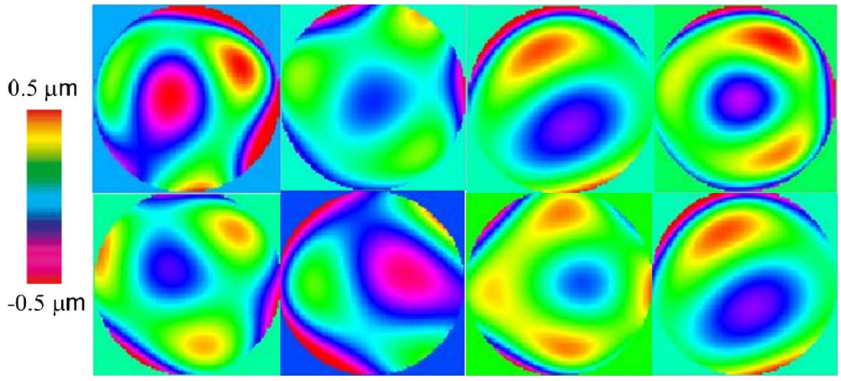

Color-coded wave aberrations for 5 mm pupil diameter in eight normal young subjects. Although the magnitude of the aberrations is similar, each eye presents distinctive spatial patterns.

normal eye with about $f/4$ aperture is approximately equivalent to less than 0.25 D of defocus, a small error typically not corrected when dealing in the clinic with refractive errors. The wave aberration of the eye can be measured using a variety of different subjective and objective techniques. A brief review of some of the technologies is presented in Appendix B. For a 5 mm pupil diameter, the root mean squared (RMS) of the wave aberration is around 0.25 μm. Figure 8 shows examples of wave aberrations in several normal eyes. Although on average the amounts of aberrations are similar, each eye has specific spatial features.

If compared with the standards of quality used in artificial optical systems, this represents poor performance. According to the Maréchal criterion, a system is effectively corrected if the wavefront error is smaller than $\lambda/14$. For a central visible wavelength, this is equivalent to 0.04 μm, a value 6 times lower than that found in a typical eye. These numbers can explain the famous quote by Helmholtz referring to the poor quality of the eye's optics [7]: "*Now it is not too much to say that if an optician wanted to sell me an instrument which had all these defects (those of the human eye), I should think myself quite justified in blaming his carelessness in the strongest terms, and giving him back his instrument*." However, Helmholtz knew perfectly that the optics of the eye was actually well adapted to serve the visual system. In fact, it is very illustrative to read his next sentence: "*Of course, I shall not do this with my eyes, and shall be only too glad to keep them as long as I can—defects and all. Still, the fact that, however bad they may be, I can get no others, does not at all diminish their defects, so long as I can maintain the narrow but indisputable position of a critic on purely optical grounds.… All these imperfections would be exceedingly troublesome in an artificial camera and in the photographic picture it produced. But they are not so in the eye—so little, indeed, that it was difficult to discover some of these…*"

2.4. The Eye Is a Nearly Aplanatic System

An optical system is considered as strictly aplanatic if spherical aberration and coma are simultaneously corrected. Despite the relatively low optical quality of the eye, it is optimized and behaves approximately as an aplanatic system. The two optical components have features that render an improved system. Indeed,

Figure 9

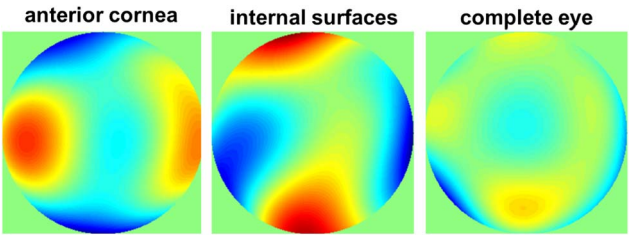

Color-coded wave aberrations for 5 mm pupil diameter for the cornea, internal surfaces (lens), and the whole eye corresponding to the right eye of the author. The lens aberrations compensate partially those present in the cornea. Adapted from J. Vis. **1**(1):1, 1–8 (2001) [11].

there is a long history of efforts to understand the relative optical contribution of the cornea and lens. Thomas Young in 1801 neutralized the corneal contribution by immersing his eye in water and found that his astigmatism persisted [8]. Today it is commonly accepted that the lens compensates for some moderate amounts of corneal astigmatism. El Hage and Berny [9] measured the corneal spherical aberration by using a photokeratoscope and the eye's spherical aberration with a Foucault-knife-edge test. They showed that the values for the cornea were more positive than those for the total eye, which was the result of the negative values for the lens spherical aberration. More recently, we also observed a coupling of other higher order aberrations between cornea and lens. Figure 9 shows wavefront aberrations for the right eye of the author for the anterior cornea, internal optics, (mostly the lens) and the complete eye. A simple inspection of these maps indicates the role of the lens to partially compensate for some of the corneal aberrations. In addition to the spherical aberration, the horizontal corneal coma was mostly compensated by the crystalline lens [10,11].

The compensation of horizontal coma is linearly related to the angle kappa of the eye, which tends to be larger for hyperopic subjects than for myopes. The larger the angle, the larger will be the corneal coma and the lens coma but with opposite signs. This indicates that the eye has a certain optical mechanism that makes it relatively insensitive to the range of values of angle kappa. A combination of surfaces curvatures, surface asphericity, and gradient index generate the negative spherical aberration in the lens required to partially balance the cornea. The corresponding values of coma for the shape factors of the cornea (around 1.2) and the lens (around −0.25) have opposite signs. This indicates that the cornea and the crystalline lens generate coma with opposite signs in the presence of field angle. If the angle increases, coma increases as well, but with sign for the lens opposite to that for the cornea.

This special design of the human eye is able to keep the eye with a rather stable optical quality independent of some alignment variables [3,12,13]. Probably nature imposed some limitations in terms of the alignment design for the eye, but the choice of the lens shapes, from an optical point of view, is optimized.

An interesting aspect is the evolution of the optics of the eye during normal aging. Aberrations tend to increase mainly due to a disruption in the coupling of the cornea and lens aberrations with age [14,15]. It could be said that the young eye is more aplanatic than the older one.

The eye behaves approximately as an aplanatic optical system, with the lens partially correcting for the spherical aberration and coma induced by the cornea.

2.5. Relative Impact of Defocus and Aberrations in the Eye's Image Quality

The interest in the higher order aberrations should not mask an important reality. Defocus is the main source of degradation in the retinal images in most persons. Figure 10 shows a realistic example of retinal images of letters in a normal eye calculated for different optical conditions. The visual object is the group of letters "play" subtending 10 arc min. This corresponds approximately to a letter size of a decimal visual acuity of 0.5 (20/40 as a Snellen fraction or 0.3 logMAR). The panels show the retinal images for a perfect eye (diffraction-limited), an eye with a normal amount of aberrations, and the same eye when a defocus of

Figure 10

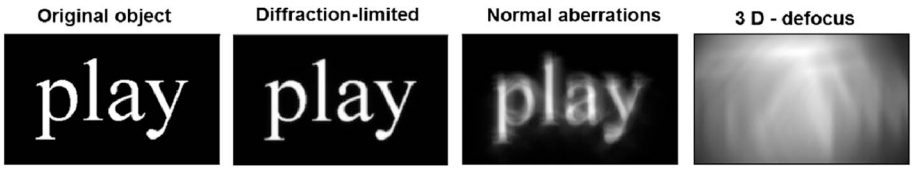

Example of retinal images of letters in a normal eye calculated for different optical conditions: diffraction-limited eye, normally aberrated, and 3 D defocus. The visual object (group of letters "play") subtends 10 arc min.

Figure 11

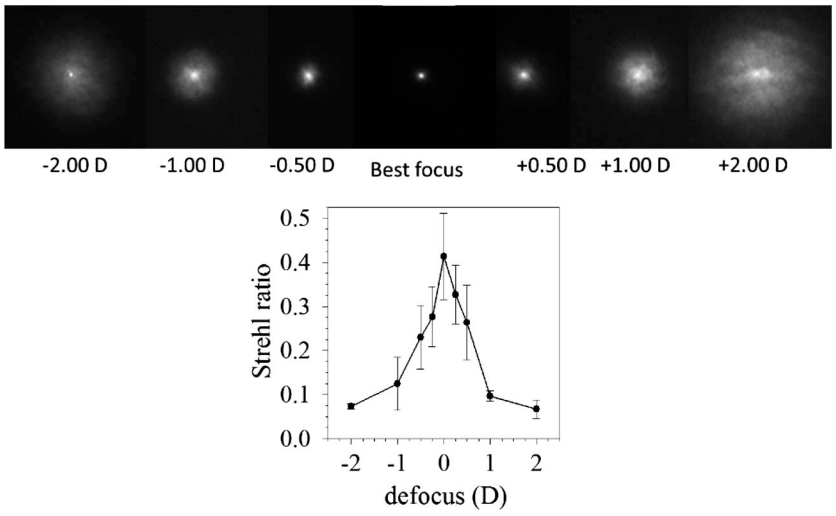

Double-pass retinal images (top) and the corresponding Strehl ratio as a function of defocus (bottom). Adapted from Optom. Vis. Sci. **79**, 60–67 (2002) [17].

3 D is added. The calculations of this example were performed for a pupil diameter of 4.8 mm.

To experimentally determine the impact of defocus, we recorded the double-pass retinal images of a point source [16] for different values of added defocus in several normal eyes [17]. Figure 11 shows the retinal images (top) and the corresponding Strehl ratios as a function of defocus (bottom). These two figures further emphasize the impact of defocus as compared with the normal aberrations. The relative impact of aberrations on image quality is comparable only for amounts of defocus below 0.25 D.

3. Impact of the Eye's Optics on Visual Performance

While the assumption that degradations in the retinal image quality imply a reduction in spatial vision holds, there are different scenarios to explain how the eye's optics actually impact vision. In this section, several factors are considered separately following the results of different experiments. A useful type of instrument to perform these studies is based on adaptive optics. Appendix C provides a short summary of this technology.

3.1. Defocus and Astigmatism

Defocus has a major impact on retinal image quality, and therefore it is also the main cause of degradation of visual acuity. Figure 12 shows visual acuity as a function of induced defocus determined in the same group of subjects for which the double-pass images were recorded (Fig. 11). There is a range of defocus around (±0.25 D) that has small impact in visual acuity. For larger values of defocus, visual acuity drops quickly. A similar behavior occurs with astigmatism.

We have recently studied [18] how small amounts of natural astigmatism below 0.5 D, and their correction, affect visual acuity (VA) in 54 normal young eyes with astigmatism ranging from 0 to 0.50 D. Astigmatism was corrected for natural pupil diameters using a crossed-cylinder device. We did not find a significant

Figure 12

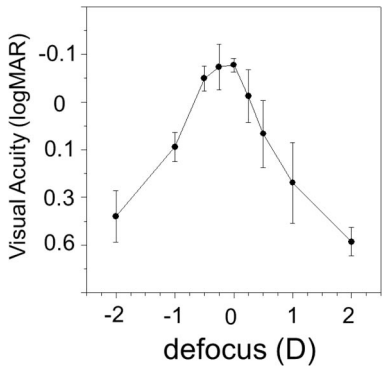

Visual acuity, expressed as logMAR, as a function of induced defocus determined in the same group of subjects where the double-pass images were recorded (Fig. 11). Adapted from Optom. Vis. Sci. **79**, 60–67 (2002) [17].

Figure 13

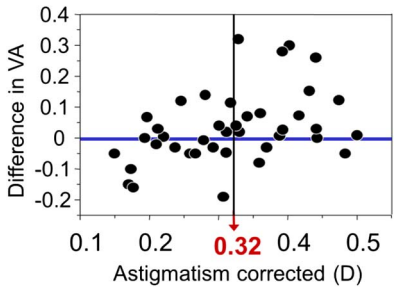

Differences in decimal visual acuity before and after correction of astigmatism as a function of the amount of corrected astigmatism. VA: visual acuity. Adapted from J. Cataract Refract. Surg. **40**, 13–19 (2013) [18].

correlation between the amount of astigmatism and visual acuity. In normal eyes, visual acuity did not depend on the precise value of astigmatism when astigmatism was below 0.50 D. Although there was some individual variability, the correction of astigmatism smaller than 0.3 D did not produce any improvement in visual acuity. Some subjects experience a small reduction in acuity after correction. Figure 13 shows the differences in visual acuity before and after careful correction of astigmatism. These results have some practical implications when determining the optimal correction of astigmatism equal to or below 0.50 D. We expect a relative improvement in visual acuity when correcting amounts of astigmatism higher than 0.3 D. However, it should be considered that this would be the case when the axis orientation of the correction is perfect. An error of 10 deg in axis causes a residual astigmatism of 35% with a change in the orientation of 40 deg and an additional defocus of half the remaining astigmatism. For example, if we want to correct 0.50 D of astigmatism, the error of 10 deg will leave a residual astigmatism of 0.17 D with the axis rotated 40 deg and an induced defocus of +0.09 D. According to these results, it is not surprising that, in clinical practice, correcting lenses are offered only in 0.25 D intervals, and astigmatism smaller than 0.25 D is rarely corrected.

3.2. Monochromatic Aberrations

When higher order aberrations are considered, the general consensus is that eyes with large amounts of aberrations present reduced visual acuity. Examples of these cases are keratoconic eyes with abnormal corneal shapes. Figure 14 shows the visual acuity measured in a group of normal and highly aberrated eyes as a function of the amount of aberrations, expressed as the RMS wavefront aberration. While there is a clear tendency of a reduced visual acuity as aberrations increases over 0.25 μm, the impact of normal amounts of aberrations (below or around that value) was not as clear. In the range considered as normal aberrations, there are at least three possible scenarios that may explain the relationship between the magnitude of the aberrations and visual acuity.

(i) The lowest the amount of the eye's aberrations, the best visual performance. As a consequence, a diffraction-limited eye would produce the highest visual acuity.

(ii) A specific type and amount of aberrations (different from zero) would produce the best performance.

Figure 14

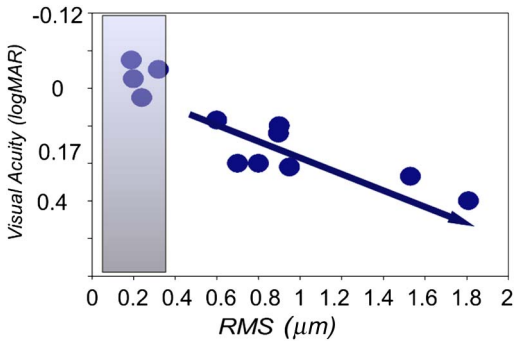

Visual acuity measured in a group of normal and highly aberrated eyes as a function of the amount of aberrations, expressed as the RMS in micrometers.

(iii) The normal (personal) aberrations, if they are within normal values, would produce the best visual acuity.

To better understand this important issue on how the aberrations impact spatial vision, we performed an experiment where we measured visual acuity and eye's aberrations in a group of normal young subjects under controlled conditions [19]. In the rest of this section, some of the most relevant results of this study are presented. Figure 15 shows the RMS of the aberrations as a function of visual acuity. The amount of aberrations varied between 0.1 and 0.7 μm across subjects within a large range of visual acuities. But subjects with the highest acuity did not have necessarily the lowest amount of aberrations. In addition, we did not find any eye with a performance near to diffraction-limited for the considered pupil diameters (average 6.5 mm). These results did not support the case of scenario (i), since those subjects with the lowest amount of aberrations did not necessarily attain the highest visual acuity.

On the other hand, it had been speculated that some aberration patterns, in particular vertical coma, would be best suited to provide good visual performance. In our study, the magnitude of coma was not correlated with acuity, so we

Figure 15

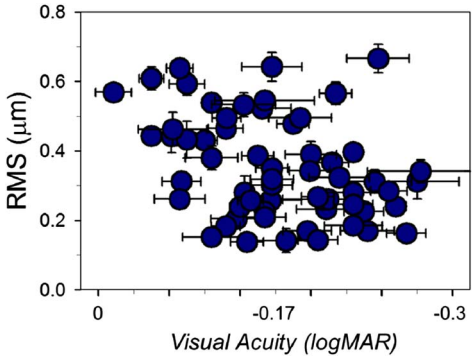

RMS of the aberrations as a function of visual acuity. The amount of aberrations varied between 0.1 and 0.7 μm across subjects within a large range of visual acuities (0 to −0.3 logMAR, equivalent to 1 to 2 decimal acuity). Adapted from Invest. Ophthalmol. Vis. Sci. **49**, 4688–4696 (2008) [19].

Figure 16

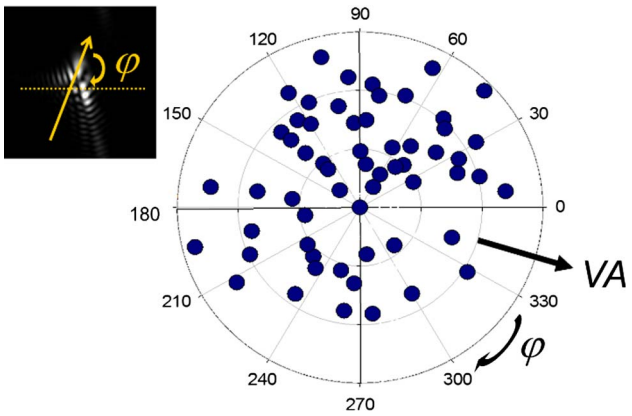

Orientation of coma as a function of visual acuity. Visual acuity ranges from 0 to −0.3 logMAR (equivalent to 1 to 2 decimal).

analyzed coma orientation as a function of visual acuity in those subjects with a magnitude of coma higher than 0.1 μm (Fig. 16). We did not find a preferred orientation of coma that could be associated with higher acuity. Similar results were also obtained for other aberrations terms, such as trefoil, and, therefore, the results did not support the ideas of scenario (ii): a particular aberration would provide the best performance.

In eyes with normal optical quality, there was not a relationship among the amount of aberrations and acuity. Moreover, subjects with the best acuity had not necessarily the best optical quality by any metrics. This suggests that the normal pattern of aberrations may provide the best performance, supporting a neural adaptation mechanism to the aberrations [20]. Our results supported those findings. If subjects adapt to their specific aberration patterns, it is quite reasonable that different amounts of aberrations would have a similar effect on vision. Although the effect of neural adaptation is probably not large, it may contribute to the robustness of the visual system, leading to a similar performance in subjects with different ocular optics quality.

In eyes with normal optics, there is not a relationship between the amount of aberrations and visual acuity.

3.3. Chromatic Aberrations

Chromatic aberrations arise from the dependence of refractive index on wavelength. They are traditionally divided into longitudinal chromatic aberration (LCA) and transverse chromatic aberration (TCA). In the eye, the former is the variation of axial power with wavelength, while the latter is the shift of the image with wavelength. Both have a significant presence in the human eye and contribute to limit the actual retinal image quality of the eye since real scenes are usually seen in white light. Figure 17 shows the LCA measured in three normal subjects using a polychromatic Hartmann–Shack wavefront sensor [21,22] and that predicted with a simple water eye model [23].

Figure 17

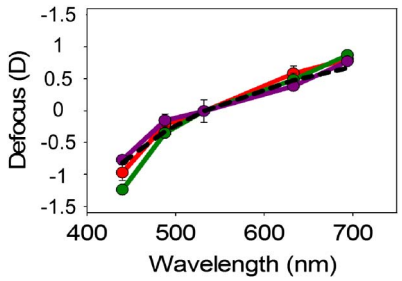

LCA measured in three normal subjects (green, red, and purple lines) and the prediction of a chromatic eye model (dashed black line). Adapted from Opt. Express **16**, 7748–7755 (2008) [22].

It should be noted that the chromatic difference in defocus for the eye is quite large, around 2 D across the visual spectrum. Figure 18 shows, as an example, a simulation of a retinal image in both monochromatic (left panel) and polychromatic light (right panel). The white-light image was obtained to include the effect of both longitudinal and lateral chromatic aberrations and shows the color degradation at the retinal plane. However, the real impact of chromatic aberration is smaller than the equivalent of 2 D defocus blur. The reason is that the visual system is equipped with a series of mechanisms to minimize the impact of chromatic aberrations. The relatively larger filtering of blue light in the lens and the macular pigment together with the spectral sensitivity of the retina reduces the contribution of the most defocused bluish colors. But despite the relatively small effect, it seems possible that the correction of chromatic aberration using achromatizing lenses would have some impact on spatial vision.

We used an adaptive optics instrument to evaluate the effect of correcting LCA combined with spherical aberration [24]. The correction of spherical aberration alone provided a larger impact than LCA in contrast sensitivity. This could be due to the pupil diameter selected for the experiments: a relatively large 4.8 mm pupil. For smaller pupil diameters, LCA correction alone could have a greater impact than correcting spherical aberration. Chromatic and spherical aberrations depend differently on the pupil diameter. The wavefront error of the spherical aberration depends on the fourth power of the radius, while LCA depends on the radius squared. When considering a lens that corrects ocular LCA outside of the eye [25], it is well known that the improvement provided in visual performance is particularly susceptible to alignment errors. In particular, a decentered LCA

Figure 18

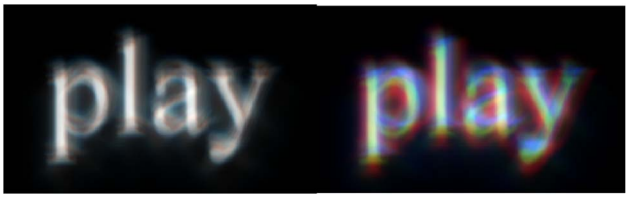

Simulation of retinal images in both monochromatic (left image) and polychromatic light (right image). The latter was obtained including the effect of both longitudinal and lateral chromatic aberrations.

corrector would add a significant amount of TCA. Misalignments of the optical axis of the lens with respect to the visual axis lead to chromatic parallax, which reduces the quality of vision measured through such a lens. The use of this type of external chromatic correctors is probably not practical, although an implementation at a fixed position, for instance, with intraocular lenses, could provide some visual improvements. More recently, the impact of chromatic aberrations in binocular visual acuity was further studied [26]. Although spherical aberration correction in monochromatic light had a greater impact monocularly than binocularly, bilateral correction of both spherical aberration and LCA may further improve binocular spatial visual acuity. This could support the use of aspheric–achromatic ophthalmic devices to improve vision.

3.4. Intraocular Scatter

Intraocular light scattering originates from localized irregularities of the refractive index within the ocular media and leads to the spread of the light at large angles over the retina. This effect is usually described by the angular distribution of the light intensity in the image plane. Although aberrations and scatter are often treated separately due to their different origins, they contribute in combination to the retinal image. Figure 19 shows schematic examples of retinal images with the contribution of both factors. Intraocular scattering may have a significant impact on retinal image contrast when the eye is observing scenes in which bright light sources are present. An example of such a condition is vision during night driving. In general, scattered light reduces retinal image quality due to a decrease in the contrast of the retinal images. An abnormal condition with elevated amount of scatter [27] severely affecting vision is cataract (Appendix D summarizes some information on cataracts).

An interesting, but not well known, fact is that aberrations and scattering interact. It was shown [28] that contrast sensitivity was reduced less by scattering when spherical aberration was present. Figure 20 shows a parameter describing the relative contrast sensitivity with and without the addition of 0.15 μm of spherical aberration in four subjects (see [28] for additional details of the experiment). This could be regarded as a type of compensatory mechanism, since with scatter, the addition of spherical aberration under certain conditions may slightly

Figure 19

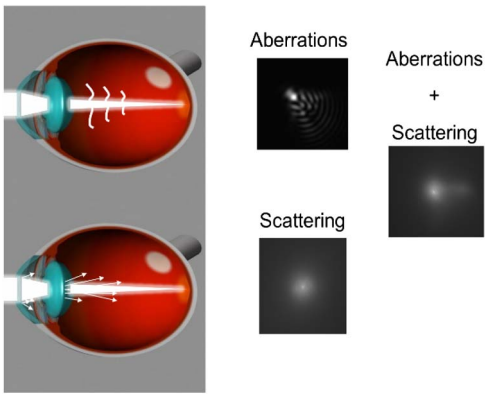

Schematic examples of retinal images of a point source showing the relative contribution of aberrations and scattering.

Figure 20

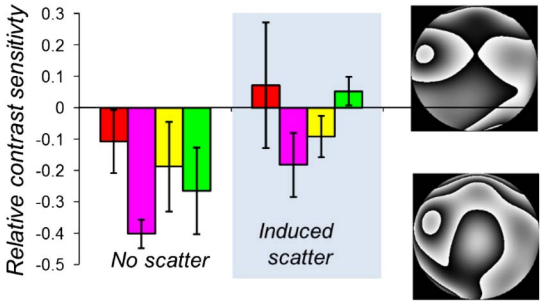

Relative contrast sensitivity in four subjects with and without the addition of 0.15 μm of spherical aberration (examples of wavefront aberrations for one of the subjects for the two conditions). Without scatter, spherical aberrations always reduce contrast sensitivity (left bars). In the presence of scatter in some subjects, the induction of spherical aberration may increase sensitivity. Relative contrast sensitivity is defined as the normalized difference of contrast sensitivity with and without spherical aberration. Adapted from J. Vis. **9**(3):19, 1–10 (2009) [28].

improve image contrast. Although the visual effect is rather small, we can suggest that the combined presence of spherical aberration and scatter in the older eye could offer a mild protective compensatory mechanism reducing the impact that the two factors may have on contrast vision separately.

It should be noted that there are many other compensatory mechanisms in the eye's optics that help to keep good vision during the lifespan. For example, while with age the eye's aberrations increase, the average pupil diameter decreases, reducing the impact of aberrations [29].

3.5. Neural Adaptation to the Aberrations

The visual system circuitry may improve our perception of the world despite the blur present in the retinal image produced by the eye's optics. If the brain adjusts for the particular eye's aberrations, vision should be clearest when looking through the normal aberrations rather than through a different optics that would be unfamiliar. Neural adaptation and plasticity are known to play a role in many important visual tasks, such as the mechanisms of blur adaptation [30] or the adaptation to field distortions. To determine if the visual system was actually adapted to the optical aberrations, we performed an experiment of subjective blur matching with the normal and rotated aberrations using an adaptive optics instrument [20]. The adaptive optics system consisted of a real-time wavefront sensor to measure the eye's aberrations and a deformable mirror to modify the aberrations. A visual channel presented stimulus to the subject. By using this instrument (see Appendix C), we rotated the aberrations (and the PSFs) of the subject while keeping the same magnitude. Subjects were asked to view a binary noise stimulus through the system with their own aberrations or with a rotated version of their aberrations. The stimulus was seen alternatively for 500 ms with both the normal and the rotated PSF, and the subject's task was to adjust the magnitude of the aberrations to match the subjective blur of the stimulus to that seen when the wave aberration was in the normal orientation. Figure 21 shows an example of the procedure. In all the subjects, the

Figure 21

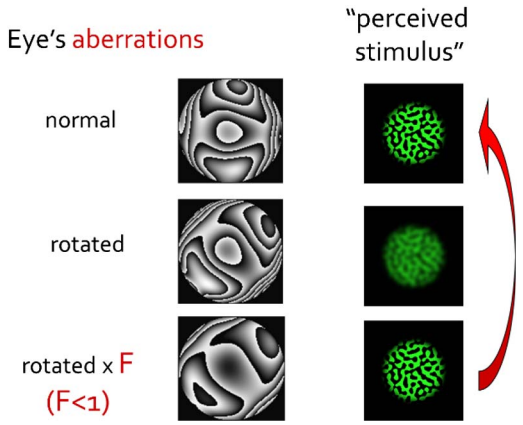

Graphical description of the procedure in the experiment to test the adaptation to aberrations. The subject is presented with a stimulus with normal aberrations and with the aberrations "rotated." If the perceived contrast is lower, the subjects adjust the amount of the rotated aberrations until the contrast for the two conditions is matched. Adapted from J. Vis. **4**(4):4, 281–287 (2004) [20].

wavefront error of the rotated wave aberration required to match the blur with the normal wave aberration was found to be less than in the normal oriented aberration case (Fig. 22). This indicates that the subjective blur for the stimulus increased significantly when the PSF was rotated. We also measured visual acuity for different aberration profiles.

Figure 23 shows an example of visual acuity measured in one subject expressed as logMAR without any aberration, with the normal aberrations and with the rotated aberrations. The performance was lowest with the rotated version of the aberrations.

An important issue that requires further research is the temporal characteristics of the adaptation process. The implications would be very different if the adaptation lasted seconds, hours, or months. Although it is obvious that the

Figure 22

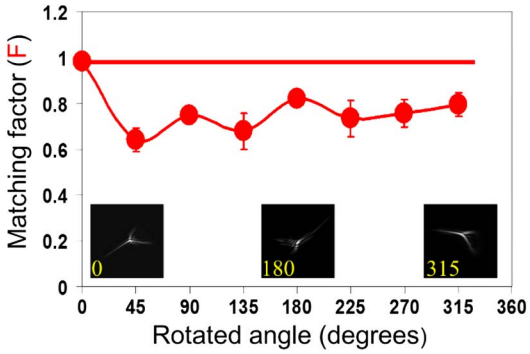

Matching factor as a function of the angle of rotation of the presented aberrations. In all subjects, the wavefront error of the rotated wave aberration required to match the blur with the normal wave aberration was found to be less than in the normal oriented aberration case. Adapted from J. Vis. **4**(4):4, 281–287 (2004) [20].

Figure 23

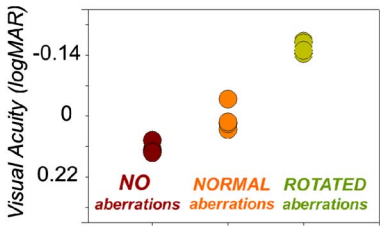

Visual acuity measured in one subject (the author) expressed as logMAR without any aberration, with the normal aberrations, and with the rotated aberrations. The performance was lowest with the rotated version of his aberrations.

visual system cannot deal with a very large amount of aberrations, it is relevant to understand the amount of aberrations that are required to induce the adaptation and its practical role in vision.

3.6. Peripheral Aberrations

In the periphery of the retina, the ability to discriminate small objects decreases severely with eccentricity. This can be due to both optical and neural factors: the eccentric angle induces optical aberrations, which lower the contrast of the retinal images, and the density of cones and ganglion cells also declines with eccentricity, resulting in sparse sampling of the image. While in central vision the optics of the eye may be the main limiting factor, in peripheral vision it is the reduced neural spatial functionality. Outside the fovea, gratings can be detected even when their orientation cannot be identified. This indicates that resolution acuity is worse than detection acuity as a result of the aliasing. This is the misinterpretation of spatial frequencies above the Nyquist limit as lower, distorted frequencies [31], by a coarse neural sampling density.

Several instruments have been used to measure peripheral optics [32,33]. The main optical deterioration in the peripheral retina is due to oblique astigmatism and field curvature. It was shown [34] that the eye's optics do not limit grating resolution in the periphery. Equivalently, high contrast visual acuity in the periphery cannot be improved with optical corrections. However, it is interesting to know that our natural peripheral optics is improved by the gradient index structure of the crystalline lens. In a recent study [35], we compared the peripheral image quality in the eyes of patients with one eye implanted with a monofocal intraocular lens and the fellow eye still with the natural pre-cataract lens. The eyes implanted had more astigmatism in the periphery than the normal eyes. This suggests that the crystalline lens provides a beneficial effect to partially compensate off-axis astigmatism.

3.7. Low Luminance Conditions

The visual system exhibits an extraordinarily high dynamic range covering more than 10 log units in luminance. There are changes occurring to the eye in dim light: the pupil sizes increases and a phenomenon called night myopia [36] may occur.

Since spatial visual performance is considerably lower at low than at higher luminance, an interesting question is whether the eye's optics still limit

Figure 24

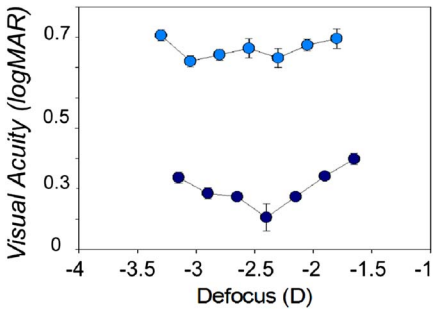

Visual acuity as logMAR measured in one normal subject for two luminance levels: 100 cd/m^2 (dark blue symbols) and 0.03 cd/m^2 (light blue symbols).

Figure 25

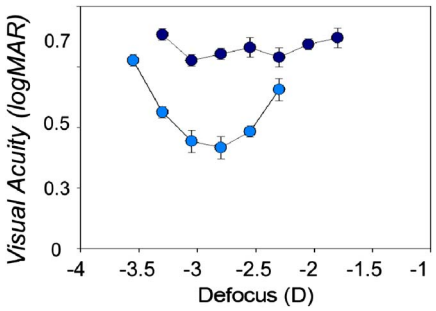

Visual acuity as logMAR measured in the same subject as Fig. 24 for the low luminance level (0.03 cd/m^2) with (light blue symbols) and without (dark blue symbols) correction of the aberrations.

performance at low light levels. We performed some experiments to address this issue. Figure 24 shows visual acuity for one subject as a function of defocus at two luminance levels (100 and 0.03 cd/m^2). As is well known, visual acuity severely decreases at low light levels. We repeated the same measurement at low luminance with the eye's aberrations corrected using an adaptive optics system. Figure 25 shows the new values of visual acuity for this case. We found that the correction of aberrations improved visual acuity in low luminance. However, other studies showed a modest improvement in contrast sensitivity after aberration correction at low light levels [37].

In an earlier experiment using an adaptive optics instrument [36], we showed that myopic shifts were modest and occurred only at very low light conditions and after dark adaptation. While clinically, defocus values as small as −0.50 D can produce visual symptoms, such refractive errors are exceeded in night myopia only under unusually low light conditions.

4. Other Related Topics and Conclusions

There are other important topics related to the eye and vision that I did not cover here. In normal subjects, binocularity related to summation and stereopsis depends on the optical quality of each eye [38]. In presbyopic subjects, combinations of different defocus in each eye, clinically called "monovision," allows us

to see binocularly at different distances, although stereoacuity is compromised due to the disparity for the two retinal images. The presence of different higher order aberrations in the two eyes may also affect vision, although at a lesser extent.

This tutorial was centered around normal eyes of subjects with normal vision. The situation in patients with different optics or with retinal pathologies would obviously be different. For example, when dealing with patients affected by age-related macular degeneration, some particular optics, such as intraocular telescopes, could help their vision.

I considered only the stationary characteristics of the eye optics. However, the eye is a living dynamic system. The temporal properties of the ocular aberrations have been studied [39] and may play an important role in the mechanism of accommodation. Eye movements are fundamental to locating the area of the retina with highest resolution within the visual objects of interest. Subjects perform rapid saccadic movements continuously. After such movements, the retinal image can be blurred due to the wobbling of the crystalline lens [40]. The implication of this oscillation for vision is probably minimized by the phenomenon of post-saccadic suppression.

A detailed understanding of the optical properties of the normal eye, and their relationship with vision, has impact in the development of new ophthalmic instrumentation. During the past decades there has been a change of paradigm in this area, especially in the design of intraocular lenses (IOLs). These lenses are implanted to replace the natural crystalline lens during cataract surgery (see Appendix D). Initially, IOLs were designed to have optical quality as good as individual lenses. However, an optimum design should mimic the young crystalline lens. Aspheric IOLs [41] with negative spherical aberration to cancel that of the eye are now widely available and represent a clear step forward. Any ophthalmic correction, from contact lenses to laser corneal ablation, will benefit from the advancements in visual optics.

New optical gadgets for video games or augmented reality will be, at some point, coupled with the eyes. In that sense, any optical engineer would benefit from a basic understanding of the eye and vision. I hope that this tutorial serves as a starting point in that direction.

Appendix A: Definitions of Angles

According to Emsley [42], the first definition of angle kappa was given by Landolt as "*the angle between the visual axis and the central pupillary line (the pupillary axis)*." This definition involved the visual axis, as the line connecting the fixation point with the object nodal point of the eye. This is not the same as the line of sight that connects the center of the entrance pupil and the fixation point. Therefore, this definition is not the one that was used by Le Grand. Angle lambda was defined by Lancaster (cited in Le Grand [1]) as the angle between the pupillary axis and the line of sight. However, Le Grand redefined the angle kappa as the angle lambda defined by Lancaster. The reason was that he understood the term visual axis in Landolt's original definition of kappa as the line of sight, since the nodal point in the eye is a paraxial theoretical concept that cannot be measured. In the words of Le Grand: "*it is not very logical to confuse geometric and fictitious ideas (optical and visual axis) and experimental ideas*

(pupillary axis and the principal line of sight)." Therefore, Le Grand maintained the old name of kappa but with the modern definition of lambda by Lancaster.

Appendix B: Methods to Measure the Eye's Aberrations

There are different techniques to estimate ocular aberrations, based on both subjective and objective methods. Subjective approaches are based on collecting visual responses by subjects, while objective methods do not require their collaboration and rely on recording images after double-pass through the ocular media. Some of the techniques proposed during the years are the method of "Vernier" alignment [43], the aberroscope [44], the Foucault-knife technique [45], and phase-retrieval calculations from double-pass retinal images [46].

The most widely used method today to measure the aberrations of the eye is the Hartmann–Shack wavefront sensor [47]. This system is based on the Hartmann test [48], as modified by Shack and Platt [49]. It consists of a microlens array, optically conjugated with the eye's pupil, and a camera placed at the array's focal plane. If a plane wavefront reaches the microlenses, a perfectly regular mosaic of spots is recorded by the camera. However, if a distorted (i.e., aberrated) wavefront reach the microlenses, the pattern of spots will be irregular. The displacement of each spot from the reference position is proportional to the derivative of the wavefront over each microlens area. From the images of Hartmann–Shack spots, the wave aberration is then retrieved.

Appendix C: Adaptive Optics Instruments

Adaptive optics is a technique originally developed in astronomy to remove the effect of atmospheric turbulence from telescope images. It has been adapted to be used in the human eye in the past two decades. One initial application was to obtain high-resolution images of the retina, allowing the discrimination of individual photoreceptors and other retinal cells *in vivo* [50–52]. Another application is to produce controlled optical aberration patterns in the eye, enabling new experiments to, for example, understand better the impact of the eye's optics on vision. This is the approach used in several of the experiments described in this tutorial. Adaptive optics instruments consist of a wavefront sensor to measure the eye's aberrations in real time and a correcting device, either a deformable mirror or a liquid crystal spatial light modulator, to modify the optics. A screen or microdisplay presents visual stimuli to the eye. More recently, binocular versions of the adaptive optics instrument for visual testing have also been developed [53].

Appendix D: Cataracts

As a result of normal aging, the crystalline lens become less transparent, diffusing light and degrading the retinal image. The advanced stage of this situation is a condition called cataracts; the lens severely scatters the light over the retina, leading to a low quality of vision. Although there are no studies showing prevention factors, it is widely accepted that reduced UV exposure may delay cataract development. A cataractous lens causes glare, halos, vision impairments, and, in the most extreme case, blindness. The standard, and successful, treatment consists of the surgical replacement of the cataractous lens with an artificial

implant called an intraocular lens (IOL), which restores the eye's ability to form clear images on the retina. Phacoemulsification is a technique that breaks the cataractous lens by ultrasound and then those small fragments are suctioned through a small incision. An IOL is then inserted in the capsular bag. Cataract surgery is almost painless and ambulatory and is now the most common eye surgery. The World Health Organization reported that age-related cataracts are responsible for 48% of world blindness, which represents about 18 million people. This seems paradoxical considering the relatively simple surgery required. Cataract is an example of a disease in which a better understanding of the eye's optics leads to improved vision with better IOLs.

Acknowledgments

This tutorial is based on a presentation I was invited to deliver at the Optical Society of America annual meeting several years ago. More recently, I presented several versions of the talk to different audiences around the world. The topics covered and content have been influenced by the audience. On purpose, I decided to base this tutorial mostly on the research we have been doing during the past few decades. This explains the large proportion of my own experiments and references included. Every member of the team has participated in one way or another and I would like to thank them all for their help and cooperation. During the past years, my laboratory has been financed by various agencies: the Spanish Ministry of Science and Technology, the Fundación Séneca (Murcia region, Spain), and the European Research Council.

References

1. Y. Le Grand and S. G. El Hage, *Physiological Optics*, Springer Series in Optical Sciences (Springer, 1980).
2. J. Tabernero, A. Benito, V. Nourrit, and P. Artal, "Instrument for measuring the misalignments of ocular surfaces," Opt. Express **14**, 10945–10956 (2006).
3. J. Tabernero, A. Benito, E. Alcón, and P. Artal, "Mechanism of compensation of aberrations in the human eye," J. Opt. Soc. Am. A **24**, 3274–3283 (2007).
4. J. W. Goodman, *Introduction to Fourier Optics*, 4th ed. (McGraw-Hill, 2005).
5. W. J. Smith, *Modern Optical Engineering*, 2nd ed. (McGraw-Hill, 1990).
6. R. J. Noll, "Zernike polynomials and atmospheric turbulence," J. Opt. Soc. Am. **66**, 207–211 (1976).
7. H. von Helmholtz, *Popular Scientific Lectures*, M. Kline, ed. (Dover, 1962).
8. T. Young, "The Bakerian Lecture. On the mechanism of the eye," Phil. Trans. R. Soc. London **91**, 23–88 (1801).
9. S. G. El Hage and F. Berny, "Contribution of crystalline lens to the spherical aberration of the eye," J. Opt. Soc. Am. **63**, 205–211 (1973).
10. P. Artal and A. Guirao, "Contribution of cornea and lens to the aberrations of the human eye," Opt. Lett. **23**, 1713–1715 (1998).
11. P. Artal, A. Guirao, E. Berrio, and D. R. Williams, "Compensation of corneal aberrations by internal optics in the human eye," J. Vis. **1**(1):1, 1–8 (2001).

12. P. Artal, A. Benito, and J. Tabernero, "The human eye is an example of robust optical design," J. Vis. **6**(1):1, 1–7 (2006).
13. P. Artal and J. Tabernero, "The eye's aplanatic answer," Nat. Photonics **2**, 586–589 (2008).
14. P. Artal, E. Berrio, A. Guirao, and P. Piers, "Contribution of the cornea and internal surfaces to the change of ocular aberrations with age," J. Opt. Soc. Am. A **19**, 137–143 (2002).
15. E. Berrio, J. Tabernero, and P. Artal, "Optical aberrations and alignment of the eye with age," J. Vis. **10**(14):34, 1–17 (2010).
16. J. Santamaria, P. Artal, and J. Bescos, "Determination of the point-spread function of human eyes using a hybrid optical-digital method," J. Opt. Soc. Am. A **4**, 1109–1114 (1987).
17. E. A. Villegas, C. González, B. Bourdoncle, T. Bonin, and P. Artal, "Correlation between optical and psychophysical parameters as function of defocus," Optom. Vis. Sci. **79**, 60–67 (2002).
18. E. A. Villegas, E. Alcon, and P. Artal, "Minimum amount of astigmatism that should be corrected," J. Cataract Refract. Surg. **40**, 13–19 (2013).
19. E. A. Villegas, E. Alcon, and P. Artal, "Optical quality of the eye in subjects with normal and excellent visual acuity," Invest. Ophthalmol. Vis. Sci. **49**, 4688–4696 (2008).
20. P. Artal, L. Chen, E. J. Fernández, B. Singer, S. Manzanera, and D. R. Williams, "Neural compensation for the eye's optical aberrations," J. Vis. **4**(4):4, 281–287 (2004).
21. P. Prieto, F. Vargas, S. Goelz, and P. Artal, "Analysis of the performance of the Hartmann-Shack sensor in the human eye," J. Opt. Soc. Am. A **17**, 1388–1398 (2000).
22. S. Manzanera, C. Canovas, P. M. Prieto, and P. Artal, "A wavelength tunable wavefront sensor for the human eye," Opt. Express **16**, 7748–7755 (2008).
23. L. N. Thibos, M. Ye, X. Zhang, and A. Bradley, "The chromatic eye: a new reduced eye model of ocular chromatic aberration in humans," Appl. Opt. **31**, 3594–3600 (1992).
24. P. Artal, S. Manzanera, P. Piers, and H. Weeber, "Visual effect of the combined correction of spherical and longitudinal chromatic aberrations," Opt. Express **18**, 1637–1648 (2010).
25. Y. Benny, S. Manzanera, P. M. Prieto, E. N. Ribak, and P. Artal, "Wide-angle chromatic aberration corrector for the human eye," J. Opt. Soc. Am. A **24**, 1538–1544 (2007).
26. C. Schwarz, C. Canovas, S. Manzanera, H. Weeber, P. M. Prieto, P. Piers, and P. Artal, "Binocular visual acuity for the correction of spherical aberration in polychromatic and monochromatic light," J. Vis. **14**(2):8, 1–11 (2014).
27. P. Artal, A. Benito, G. M. Pérez, E. Alcón, A. De Casas, J. Pujol, and J. M. Marín, "An objective scatter index based on double-pass retinal images of a point source to classify cataracts," PLoS One **6**, e16823 (2011).
28. G. Pérez, S. Manzanera, and P. Artal, "Impact of scattering and spherical aberration in contrast sensitivity," J. Vis. **9**(3):19, 1–10 (2009).
29. A. Guirao, C. Gonzalez, M. Redondo, E. Geraghty, S. Norrby, and P. Artal, "Average optical performance of the human eye as a function of age in a normal population," Investig. Ophthalmol. Vis. Sci. **40**, 203–213 (1999).

30. M. A. Webster, M. A. Georgeson, and S. M. Webster, "Neural adjustments to image blur," Nat. Neurosci. **5**, 839–840 (2002).
31. P. Artal, A. M. Derrington, and E. Colombo, "Refraction, aliasing, and the absence of motion reversals in peripheral vision," Vis. Res. **35**, 939–947 (1995).
32. A. Guirao and P. Artal, "Off-axis monochromatic aberrations estimated from double pass measurements in the human eye," Vis. Res. **39**, 207–217 (1999).
33. B. Jaeken, L. Lundström, and P. Artal, "Fast scanning peripheral wave-front sensor for the human eye," Opt. Express **19**, 7903–7913 (2011).
34. L. Lundström, S. Manzanera, P. M. Prieto, D. B. Ayala, N. Gorceix, J. Gustafsson, P. Unsbo, and P. Artal, "Effect of optical correction and remaining aberrations on peripheral resolution acuity in the human eye," Opt. Express **15**, 12654–12661 (2007).
35. B. Jaeken, S. Mirabet, J. M. Marín, and P. Artal, "Comparison of the optical image quality in the periphery of phakic and pseudophakic eyes," Invest. Ophthalmol. Vis. Sci. **54**, 3594–3599 (2013).
36. P. Artal, C. Schwarz, C. Cánovas, and A. Mira-Agudelo, "A night myopia studied with an adaptive optics visual analyzer," PLoS ONE **7**, e40239 (2012).
37. E. Dalimier, C. Dainty, and J. L. Barbur, "Effects of higher-order aberrations on contrast acuity as a function of light level," J. Mod. Opt. **55**, 791–803 (2008).
38. E. J. Fernández, C. Schwarz, P. M. Prieto, S. Manzanera, and P. Artal, "Impact on stereo-acuity of two presbyopia correction approaches: monovision and small aperture inlay," Biomed. Opt. Express **4**, 822–830 (2013).
39. H. Hofer, P. Artal, B. Singer, J. L. Aragón, and D. R. Williams, "Dynamics of the eye's wave aberration," J. Opt. Soc. Am. A **18**, 497–506 (2001).
40. J. Tabernero and P. Artal, "Lens oscillations in the human eye. Implications for post-saccadic suppression of vision," PLoS ONE **9**, e95764 (2014).
41. A. Guirao, M. Redondo, E. Geraghty, P. Piers, S. Norrby, and P. Artal, "Corneal optical aberrations and retinal image quality in patients in whom monofocal intraocular lenses were implanted," Arch. Ophthalmol. (Chicago) **120**, 1143–1151 (2002).
42. H. H. Emsley, *Visual Optics* (Hatton, 1948).
43. M. S. Smirnov, "Measurement of the wave aberration of the human eye," Biofizika **6**, 776–795 (1961).
44. H. C. Howland and B. Howland, "A subjective method for the measurement of monochromatic aberrations of the eye," J. Opt. Soc. Am. **67**, 1508–1518 (1977).
45. F. Berny and S. Slansky, "Wavefront determination resulting from Foucault test as applied to the human eye and visual instruments," in *Optical Instruments and Techniques*, J. H. Dickenson, ed. (Oriel, 1969), pp. 375–386.
46. P. Artal, J. Santamaría, and J. Bescós, "Retrieval of the wave aberration of human eyes from actual point-spread function data," J. Opt. Soc. Am. A **5**, 1201–1206 (1988).
47. J. Liang, B. Grimm, S. Goelz, and J. F. Bille, "Objective measurement of the WA´s aberration of the human eye with the use of a Hartmann-Shack sensor," J. Opt. Soc. Am. A **11**, 1949–1957 (1994).
48. J. Hartmann, "Bemerkungen uber den Bau und die Justirung von Spektrographen," Zt. Instrumentenkd. **20**, 47–58 (1900).

49. R. V. Shack and B. C. Platt, "Production and use of a lenticular Hartmann screen," J. Opt. Soc. Am. **61**, 656 (1971).
50. A. Roorda and D. R. Williams, "The arrangement of the three cone classes in the living human eye," Nature **397**, 520–522 (1999).
51. F. Vargas-Martin, P. Prieto, and P. Artal, "Correction of the aberrations in the human eye with liquid crystal spatial light modulators: limits to the performance," J. Opt. Soc. Am. A **15**, 2552–2562 (1998).
52. A. Dubra, Y. Sulai, J. L. Norris, R. F. Cooper, A. M. Dubis, D. R. Williams, and J. Carroll, "Noninvasive imaging of the human rod photoreceptor mosaic using a confocal adaptive optics scanning ophthalmoscope," Biomed. Opt. Express **2**, 1864–1876 (2011).
53. E. J. Fernández, P. M. Prieto, and P. Artal, "Binocular adaptive optics visual simulator," Opt. Lett. **34**, 2628–2630 (2009).

Pablo Artal is Professor of Optics at the University of Murcia, Spain. He spent several periods doing collaborative research in laboratories in Europe, Australia, and the USA. He is a fellow member of The Optical Society (OSA), the European Optical Society (EOS), and The Association for Research in Vision and Ophthalmology (ARVO). He received the prestigious 2013 Edwin H. Land medal award from OSA in recognition of his scientific contributions to the advancement of diagnostic and correction alternatives in visual optics. He is the recipient of an exclusive European Research Council advanced grant. He has published more than 200 reviewed papers, which have received over 6200 citations (h-index: 43), and presented more than 150 invited talks in international meetings and around 300 seminars in different research institutions. He is also a co-inventor of 18 international patents in the fields of optics and ophthalmology. He has pioneered a number of highly innovative advances in the methods for studying the optics of the eye and has contributed substantially to our understanding of the factors that limit human visual resolution. He has been the mentor of many graduate and post-doctoral students. His science blog (http://pabloartal.blogspot.com) is followed by readers, mostly graduate students and fellow researchers, from around the world. He has been topical editor of the *Journal of the Optical Society of America A* and is currently an associate editor of the *Journal of Vision*.